Self-assembled patterns of nanospheres with symmetries from submicrons to centimeters

Kun Chen[a)]
Department of Biomedical Engineering, Northwestern University, Evanston, Illinois 60208

Allen Taflove
Department of Electrical and Computer Engineering, Northwestern University, Evanston, Illinois 60208

Young L. Kim and Vadim Backman[b)]
Department of Biomedical Engineering, Northwestern University, Evanston, Illinois 60208

(Received 4 August 2004; accepted 11 November 2004; published online 7 January 2005)

We report pattern formations during the drying of a sheet of an aqueous suspension of nanospheres. The structures self-assembled by nanospheres span several centimeters and exhibit order at scales ranging from nanometers to centimeters, although the substrate has no predefined pattern. Within these structures, several regular patterns can be identified, including two-dimensional periodic gratings generated by crack networks with a characteristic spatial frequency linearly depending on the evaporation speed, and three-dimensional flower-like structures. This phenomenon potentially provides a simple and inexpensive method to grow structures having unique electromagnetic and/or biological properties. © *2005 American Institute of Physics*. [DOI: 10.1063/1.1851002]

Colloidal particles self-assemble into a wide range of ordered structures. The dynamic formation of such structures is the outcome of underlying fundamental processes. Microscopically, the self-organization phenomenon is driven by interactions among the colloidal particles and between the particles and the substrate. These interactions include electrostatic forces, van der Waals forces, steric interactions, capillary forces, surface tension, tensile stress, and frictional force. For example, the propagation of quasistatic fracture that forms fractal-like patterns[1] and spiral cracks[2] can be simulated by means of a discrete spring-block model consisting of an array of blocks interconnected with coil springs.[1,2] Macroscopically, fluid transportation plays a central role in the ring pattern formation of dried liquid drops.[3] Depletion effects in particle suspensions produce attraction force between the spheres or between the spheres and a profiled template, thus a colloid crystal can be grown on patterned surfaces.[4,5] The crack formation in a colloid film is directly related to the stress field within the film surface,[6] which arises from the loss of water content and leads to parallel[6] or spoke-like[7] crack patterns.

In this letter, we report an experimental observation of the growth on a flat featureless surface of self-organized patterns of nanospheres on scales ranging from 30 nm to several centimeters. Here, the ratio of the upper to lower characteristic distance scales in these self-assembled structures approaches 10^6. The structures consist of several definitive two and three dimensional substructures which display new symmetries relative to the ones discussed in Refs. 6 and 7.

The experiments were conducted using aqueous suspensions of monodispersed polystyrene nanospheres (Duke Scientific, Inc.). The mean sphere size was 33 nm with a standard deviation of ~11%. The weight concentration of the aqueous suspensions was 10%. The aqueous suspension was kept in a refrigerator at 5 °C before experiments. A drop of the aqueous suspension (volume ≈30 μl) was uniformly smeared on a flat surface of a glass slide substrate by using a clean glass rod to cover the area of ~30 mm × 10 mm. The initial thickness of the suspension was ~100 μm. The evaporation process took about 10 min to form self-assembled patterns at room temperature 20.5 °C. Self-assembly of the film was repeatable as long as the propagation of a drying front was sustained. The self-assembled process was observed under an optical microscope (Olympus BX40, Optical Analysis Co.). We acquired video images at constant time intervals using a CCD camera (Coolsnap, Roper Scientific, Inc.) coupled to the microscope. The drying process was then reconstructed using the video sequence. The CCD was capable of acquiring intensity images as pseudocolor images. Each intensity image contained 696 × 520 pixels. In order to obtain the dimension of images, we calibrated the pixel size using the image acquired from 4.54 μm diameter polystyrene microspheres (Polysciences, Inc.). The size of the field of view was 165 μm × 123 μm when a 40× objective was used.

The process of evaporation was characterized by a propagating drying front (Fig. 1), followed by the tips of the longitudinal cracks. The propagation speed of the front depended on the actual evaporation rate, and we defined the propagation direction of the front as the longitudinal direction. The drying front always started at the periphery of the suspension and propagated inwards. It distinctively divided the sample into two parts, an aqueous part and a solid thin-film part. Thus, the front separated the two phases coexisting within the sample. The film was comprised of self-aggregated nanospheres. At a distance behind the drying front, spatially well-organized longitudinal cracks grew along the direction perpendicular to the drying front. The propagation speed of the drying front was reconstructed from a video sequence, captured by the microscope as the drying front swept through its field of view. The data showed that

[a)]Current address: Key Laboratory for Quantum Optics of Chinese Academy of Sciences, Center for Cold Atom Physics of Chinese Academy of Sciences, Shanghai Institute of Optics and Fine Mechanics, Shanghai 201800, China.
[b)]Author to whom correspondence should be addressed; electronic mail: v-backman@northwestern.edu

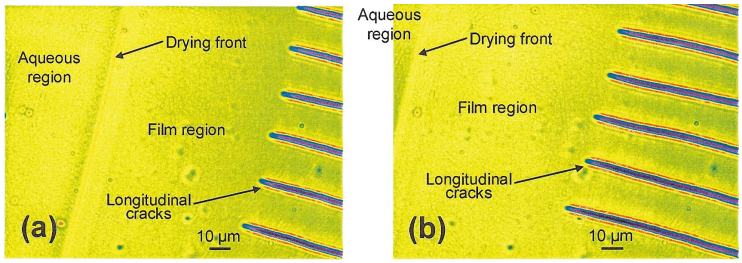

FIG. 1. (Color) pseudocolor intensity images of the propagation of the drying front and formation of the longitudinal cracks. The time elapsed from (a) to (b) is 8.815 s.

this speed was close to constant in the local area (165 μm $\times$123 μm) of the observation point. Immediately following the drying front, whose propagation speed decreased as evaporation proceeded, the solid phase of the film started to reorganize to form regular patterns. The primary pattern to emerge was a periodic grating formed by nearly parallel and equispaced crack formed within the film portion of the sample and extending along the longitudinal direction (Fig. 2). This was followed by the formation of secondary cracks in the transverse direction, which joined the neighboring longitudinal cracks, thus forming a two dimensional grid.

The longitudinal cracks were the primary fractures, long-range, perpendicular to the drying front and all originated at the periphery. They had the highest density at the periphery of the sheet and became less crowded as they approached the center. None of the longitudinal cracks have free ends, i.e. they never terminated abruptly, but always ended up on other cracks. The secondary cracks were all in short range, with most appearing as transverse cracks. Unlike longitudinal cracks, formation of transverse cracks was swift and unrelated to the propagating drying front. Each transverse crack always started at a flaw on an existing crack and grew to a flaw on a neighboring crack. According to our observation, there was a monotonic dependence between the average distance among the transverse cracks and that among the longitudinal cracks. In summary, the formation of the two dimensional crack networks is a two-step process. First, the longitudinal cracks were created by the drying front, then the system self-stabilized to a grid by the cracks in the transverse direction.

The drying process finally ended with the formation of a three-dimensional flower-like pattern at the center of the sample [Figs. 3(a) and 3(b)], which was the last to solidify. This structure consisted of multiple "petals," each $\sim$0.2 mm in the transverse direction and several millimeters long. We estimated that the number of nanospheres in each "petal" is $\sim 10^{12}$. The dynamic ripple pattern projected by a He:Ne laser beam through the flower center indicated a symmetric transport process during its formation (data not shown). The morphology of the flower structure is caused by the stress gradient in the nanosphere self-aggregation near the center. As the aqueous part of the sheet retreated to the center, the stress along the longitudinal direction reached maximum. The stress gradient pointed outwards from the center, along the radial direction. Instead of creating transverse cracks, the longitudinal stress was released by bending the film stripes into the third dimension, thereby generating a flower pattern.

Detailed data analysis has demonstrated that the spacing between the longitudinal cracks, i.e., the grating period d, depends inversely on the drying-front speed. Consequently, the spatial frequency of the longitudinal cracks $f_d \equiv 1/d$ is a linear function of the drying-front speed (Fig. 4). A linear fitting of the data demonstrates that $f_d = 0.00627\ V$, with f_d in μm^{-1} and V in μm/s. In our experiments the spatial period of the longitudinal gratings ranged from 9 to 170 μm, thus spanning almost two orders of magnitude.

Although elucidation of the exact mechanism of the pattern formation discussed here will require further studies, it is most likely that the two-dimensional periodic longitudinal cracks in the self-assembled pattern of the nanosphere suspension are in part due to tensile stress in the drying film, the universal mechanism of crack propagation. Leung and colleague have simulated the propagation of quasistatic fracture in a brittle layer in contact with a substrate using a two-dimensional spring-block model consisting of two elementary processes: stick slip action on the frictional substrate and crack propagation on the layer.[1,2] The spring-block model demonstrated the formation of fractal-like patterns over a wide range of scales. In our study, the directional force generated by the drying front can be considered an additional field of force in the spring-block model, leading to the formation of the spatially ordered longitudinal gratings.

The observed phenomena open the possibility of controlling the period of a grating from submicron to millimeter scales by varying the drying rate. For example, the evaporation process could be performed in an enclosed chamber where the diffusion rate of solvent in air could be controlled. When the partial pressure of the solvent in air reaches satu-

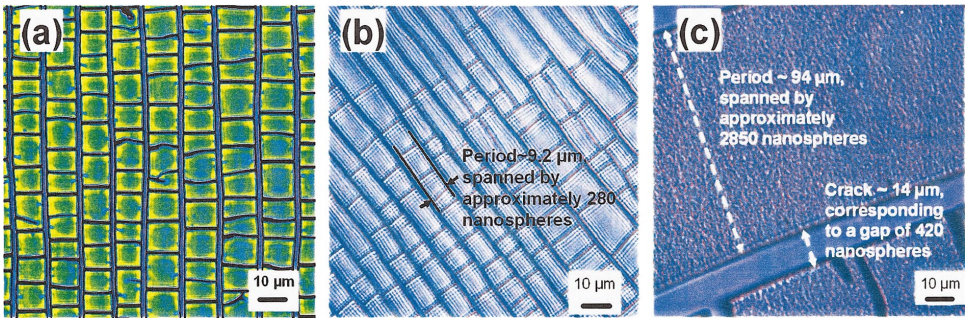

FIG. 2. (Color) structure of a typical self-assembled film: (a) pseudocolor intensity image of a film portion exhibiting a nearly periodic grating at micron scale; (b) image of the film microstructure. An estimate of the number of nanospheres spanning one period is shown; (c) detailed photograph of a single period/crack.

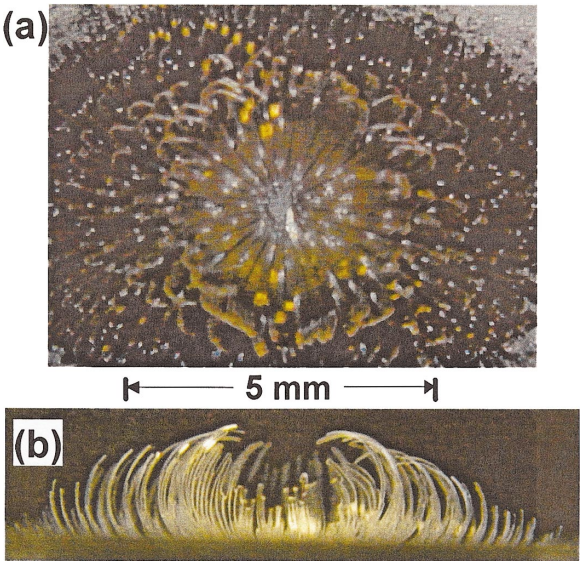

FIG. 3. (Color) flower pattern at the center of the self-assembly: (a) top-view and (b) side-view.

ration, the evaporation rate would be reduced to zero. On the other hand, the evaporation rate could be accelerated by pumping out the solvent in gaseous phase. Moreover, the drying rate could be easily controlled by varying the thickness of the suspension, its temperature, and a wide range of other parameters that affect the rate of evaporation. Extrapolating Fig. 4, by increasing the drying rate to ~150 μm/s, a 1-μm-spatial period could be achieved. The wavelength of such a period corresponds to the near-infrared. By slowing the drying rate down to 0.15 μm/s, a grating with 1 mm wavelength (i.e., approaching the radio-frequency range) could be formed.

A significant application of such self-assembled structures would be in implementing forms of an important class of periodic electromagnetic wave structures, the frequency-selective surface (FSS).[8,9] The most common type of FSS is an engineered material consisting of one or multiple thin, parallel screens of periodically distributed metal patches or apertures in a ground plane.[8] Another type of FSS, more appropriate for the present discussion, employs a lossy all-dielectric sheet that has an inhomogeneous permittivity that is doubly periodic in the lateral direction.[9] FSS can be designed to exhibit either high transmittance or high reflectance to impinging plane electromagnetic waves at specific wavelengths. Furthermore, FSS can provide a reactive, slow-wave surface that allows near-surface antennas to be realized with smaller physical dimensions than when using a metal ground plane.[10] FSS technology has important industrial, scientific, and defense applications from the cell-phone band[10] through millimeter waves[11] to the near-infrared[12] in spectral filtering and suppression of surface waves. We note that the material and technique reported here has the potential to grow a self-assembled (rather than an engineered) structure with a di-

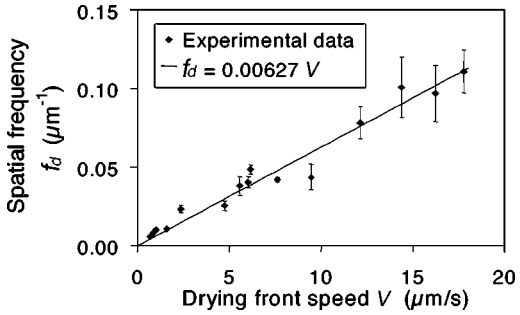

FIG. 4. Spatial frequency of the grating as a function of the drying front propagation speed.

electric periodicity varying in a single growth cycle from microns to millimeters that is maintained over centimeter-squared surface areas. Such self-assembled films could be an inexpensive means to realize tailored FSS filtering and surface-wave suppression action over bandwidths from microwaves to visible light in a single film. We foresee further possibilities for the ultra-large self-assemblies of nanospheres reported here. Specifically, doping the polystyrene suspension with metallic nanoparticles would lead to the synthesis of materials having novel electromagnetic wave interaction properties spanning microwaves through optics. For example, by appropriate selection of the dopant electrical conductivity and magnetic permeability, it may be possible to create, ultra-wideband radar absorbers (stealth technology) that cover entire surfaces of planes and ships, wherein especially in the latter case there is little present alternate technology. Furthermore, by attaching biomolecular function groups to the nanospheres, it may be feasible to create ultralarge self-assembled nanoparticle biosensor arrays for genomics and proteomics applications.

The authors thank Dr. Alexander Golovin for helpful discussions. This work is supported by US NSF Grant No. BES-0238903 and the Institute for Bioengineering and Nanoscience in Advanced Medicine of Northwestern University.

[1]K.-T. Leung and Z. Z. Néda, Phys. Rev. Lett. **85**, 662 (2000).
[2]K.-T. Leung, L. Józsa, M. Ravasz, and Z. Néda, Nature (London) **410**, 166 (2001).
[3]R. D. Deegan, O. Bakajin, T. F. Dupont, G. Huber, S. R. Nagel, and T. A. Witten, Nature (London) **389**, 827 (1997).
[4]K. Lin, J. C. Crocker, V. Prasad, A. Schofield, D. A. Weitz, T. C. Lubensky, and A. G. Yodh, Phys. Rev. Lett. **85**, 1770 (2000).
[5]Y. H. Ye, S. Badilescu, and V. Truong, Appl. Phys. Lett. **79**, 872 (2001).
[6]C. Allain and L. Limat, Phys. Rev. Lett. **74**, 2981 (1995).
[7]T. Okubo, S. Okuda, and H. Kimura, Colloid Polym. Sci. **280**, 454 (2002).
[8]B. A. Munk, *Frequency Selective Surfaces: Theory and Design* (John Wiley, New York, 2000).
[9]O. Forslund, A. Karlsson, and S. Poulsen, Report code LUTEDX/(TEAT-7101)/1-23/(2001) (Department of Electroscience, Lund Institute of Technology, Sweden, 2001).
[10]Information Sheet IS002-A (Etenna Corporation, 6100-C Frost Place, Laurel, MD 20707).
[11]S. E. Whitcomb and J. Keene, Appl. Opt. **19**, 197 (1980).
[12]M. D. Morgan, W. E. Horne, V. Sundaram, J. C. Wolfe, S. V. Pendharkar, and R. Tiberio, J. Vac. Sci. Technol. B **14**, 3903 (1996).